

# Chapter 12

## HEAD-TAIL INSTABILITIES

### 12.1 Transverse Head-Tail

Let us now consider the short-range field of the transverse impedance; i.e.,  $Z_1^\perp(\omega)$  when  $\omega$  is large. This is equivalent to replacing the discrete line spectrum by a continuous spectrum. The summation in Eq. (10.33) or Eq. (11.1) can be transformed into an integration. The coherent angular frequency for the  $m$ th azimuthal mode is therefore

$$\Omega_m - m\omega_s = -\frac{i}{1+m} \frac{ecI_b}{4\pi E_0 \omega_\beta} \int_{-\infty}^{\infty} d\omega Z_1^\perp(\omega) h_m(\omega - \omega_\xi) , \quad (12.1)$$

where  $\omega_\xi = \xi\omega_0/\eta$  is the betatron frequency shift due to chromaticity  $\xi$ ,  $\eta$  is the slip factor,  $\omega_0$  is the revolution angular frequency, and  $E_0$  is the particle energy. Note that the factor of  $M$ , the number of bunches, in the numerator and denominator cancel. This is to be expected because the perturbation mechanism is driven by the short-range wake field and the instability is therefore a single-bunch effect. This explains why we do not include the subscript  $\mu$  describing phase relationship of consecutive bunches. The growth rate, which is the imaginary part of Eq. (12.1) is given by

$$\frac{1}{\tau_m} = -\frac{1}{1+m} \frac{ecI_b}{4\pi E_0 \omega_\beta} \int_0^{\infty} d\omega \operatorname{Re} Z_1^\perp(\omega) [h_m(\omega - \omega_\xi) - h_m(\omega + \omega_\xi)] , \quad (12.2)$$

where use has been made of the antisymmetry of  $\operatorname{Re} Z_1^\perp(\omega)$ . It is clear that there can be no instability when the chromaticity is zero. When there is finite chromaticity, however,

the growth does not have a threshold. On the other hand, the tune shift, given by

$$\Delta\Omega_m = \frac{1}{1+m} \frac{ecI_b}{4\pi E_0 \omega_\beta} \int_0^\infty d\omega \operatorname{Im} Z_1^\perp(\omega) [h_m(\omega - \omega_\xi) + h_m(\omega + \omega_\xi)] , \quad (12.3)$$

does not vanish when the chromaticity is zero.

Let us demonstrate this by using the resistive wall impedance. We substitute the expression of the resistive wall impedance of Eq. (1.44) into Eq. (12.1). The result of the integration over  $\omega$  is [1]

$$\frac{1}{\tau_m} = -\frac{1}{1+m} \frac{eI_b c}{4\nu_\beta E_0} \left( \frac{2}{\omega_0 \tau_L} \right)^{1/2} |Z_1^\perp(\omega_0)| \operatorname{Re} F_m(\chi) , \quad (12.4)$$

where  $|Z_1^\perp(\omega_0)|$  is the magnitude of the resistive wall impedance at the revolution frequency. The tune shift is given by

$$\Delta\Omega_m = \frac{1}{1+m} \frac{eI_b c}{4\nu_\beta E_0} \left( \frac{2}{\omega_0 \tau_L} \right)^{1/2} |Z_1^\perp(\omega_0)| \operatorname{Im} F_m(\chi) , \quad (12.5)$$

The form factor is given by

$$\begin{Bmatrix} \operatorname{Re} F_m(\chi) \\ \operatorname{Im} F_m(\chi) \end{Bmatrix} = \frac{1}{2\sqrt{\pi}} \int_0^\infty \frac{dy}{\sqrt{y}} [h_m(y - y_\xi) \mp (y + y_\xi)] , \quad (12.6)$$

where  $h_m$  are power spectra of the  $m$ th excitation mode in Eq. (10.41) written as functions of  $y = \omega\tau_L/\pi$  and  $y_\xi = \chi/\pi = \xi\omega_0\tau_L/(\pi\eta)$ . The first term in the integrand comes from contributions by positive frequencies while the second term by negative frequencies. The form factors for  $m = 0$  to 5 are plotted in Fig. 12.1.

This single-bunch instability will occur in nearly all machines. The  $m = 0$  mode is the rigid-bunch mode when the whole bunch oscillates transversely as a rigid unit. For the  $m = 1$  mode, the head of the bunch moves transversely in one direction while the tail moves transversely in the opposite direction with the center-of-mass stationary, and is called the dipole head-tail mode. This is the head-tail instability first analyzed by Pellegrini and Sands [2, 3].

For small chromaticity phase  $\chi \lesssim 2.3$ , the integrand in Eq. (12.6) can be expanded and the growth rate becomes proportional to chromaticity. The form factor has been computed and listed in Table 12.1, where positive sign implies damping. We see from Table 12.1 that mode  $m=0$  is stable for positive chromaticity (above transition or  $\eta > 0$ ).

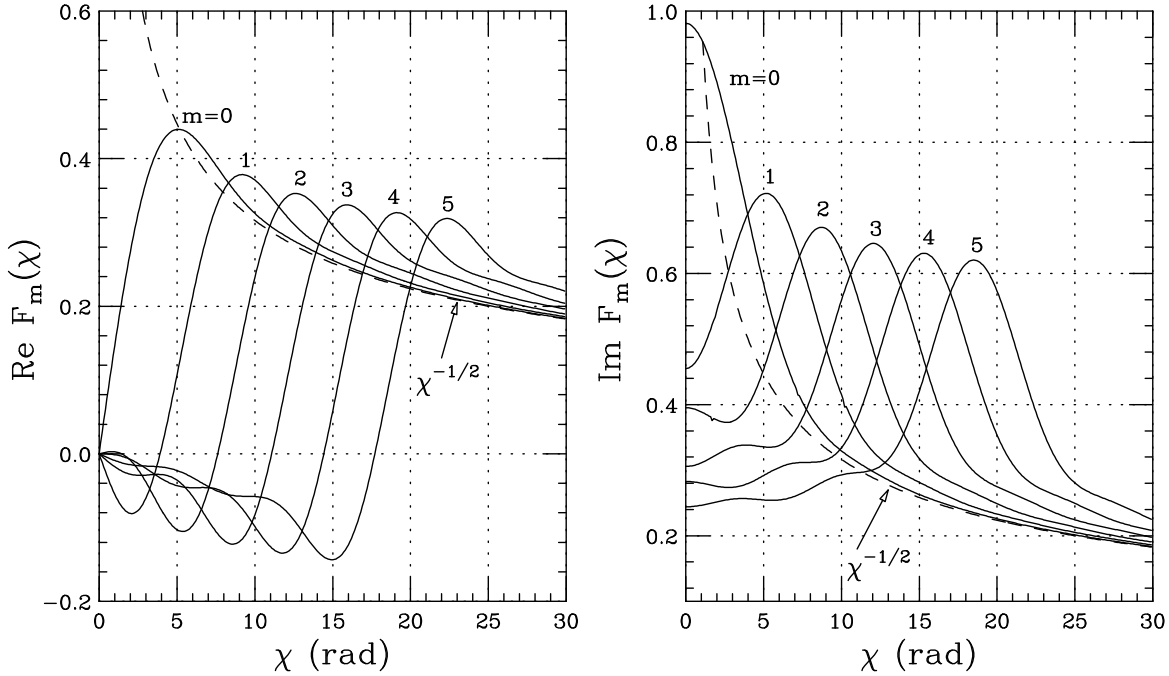


Figure 12.1: Real and imaginary parts of the form factor  $F_m(\chi)$  for head-tail instability resulting from the resistive-wall impedance, for modes  $m = 0$  to 5.

This is expected because the excitation spectrum for this mode has been pushed towards the positive-frequency side. All other modes ( $m > 0$ ) should be unstable because their spectra see relatively more negative  $\mathcal{R}e Z_1^\perp$ . Looking into the form factors in Fig. 12.1, however, the growth rate for  $m = 4$  is tiny and mode  $m = 2$  is even stable. This can be clarified by looking closely into the excitation spectra in Fig. 7.5. We find that while mode  $m = 0$  has a large maximum at zero frequency, all the other higher even  $m$  modes also have small maxima at zero frequency. As these even  $m$  spectra are pushed to the right, these small central maxima see more impedance from positive frequency than negative frequency. Since these small central maxima are near zero frequency where  $|\mathcal{R}e Z_1^\perp|$  is large, their effect may cancel out the opposite effect from the larger maxima which interact with the impedance at much higher frequency where  $|\mathcal{R}e Z_1^\perp|$  is smaller. This anomalous effect does not exist in the Legendre modes or the Hermite modes, because the corresponding power spectra vanish at zero frequency when  $m > 0$ .

A broadband resonance can also drive the head-tail instability. However, the power spectrum must be so frequency shifted by chromaticity that it overlaps with the resonance peak. For example, the  $m = 0$  mode must be shifted by negative chromaticity

Table 12.1: Linearized form factor of transverse head-tail modes driven by the resistive wall impedance when  $\chi \lesssim 2.3$ .

Mode	Form Factor
$m$	$F_m$
0	$+0.1495 \chi$
1	$-0.0600 \chi$
2	$+0.0053 \chi$
3	$-0.0191 \chi$
4	$-0.0003 \chi$
5	$-0.0098 \chi$

(above transition) so that  $\omega_\xi \approx -\omega_r$ , where  $\omega_r$  is the resonant frequency of the impedance. Mode  $m$  peaks roughly at

$$\frac{\omega\tau_L}{\pi} \approx m + 1 , \quad (12.7)$$

where  $\tau_L$  is the full bunch length. Therefore to be excited by the resonance impedance, the betatron frequency shift due to chromaticity,  $\omega_\xi$ , required is roughly given by

$$\omega_\xi = - \left[ \omega_r - \frac{\pi(m+1)}{\tau_L} \right] . \quad (12.8)$$

Although the head-tail instabilities can be damped by the incoherent spread in betatron frequency, it is advisable to run the machine at a negative chromaticity above transition. In this case, all the higher modes with  $m \neq 0$  will be stable, and the unstable  $m = 0$  mode can be damped with a damper.

Head-tail modes of oscillations can be excited by shifting the chromaticity to the unstable direction and observed using a wideband pickup. These modes were first observed in the CERN PS Booster [4] and depicted in Fig. 12.2. They have also been measured in the Fermilab rings.

## 12.2 Longitudinal Head-Tail

The transverse head-tail instability comes about because of nonzero chromaticity or the betatron tune is a function of energy spread. Most important of all, the introduction of

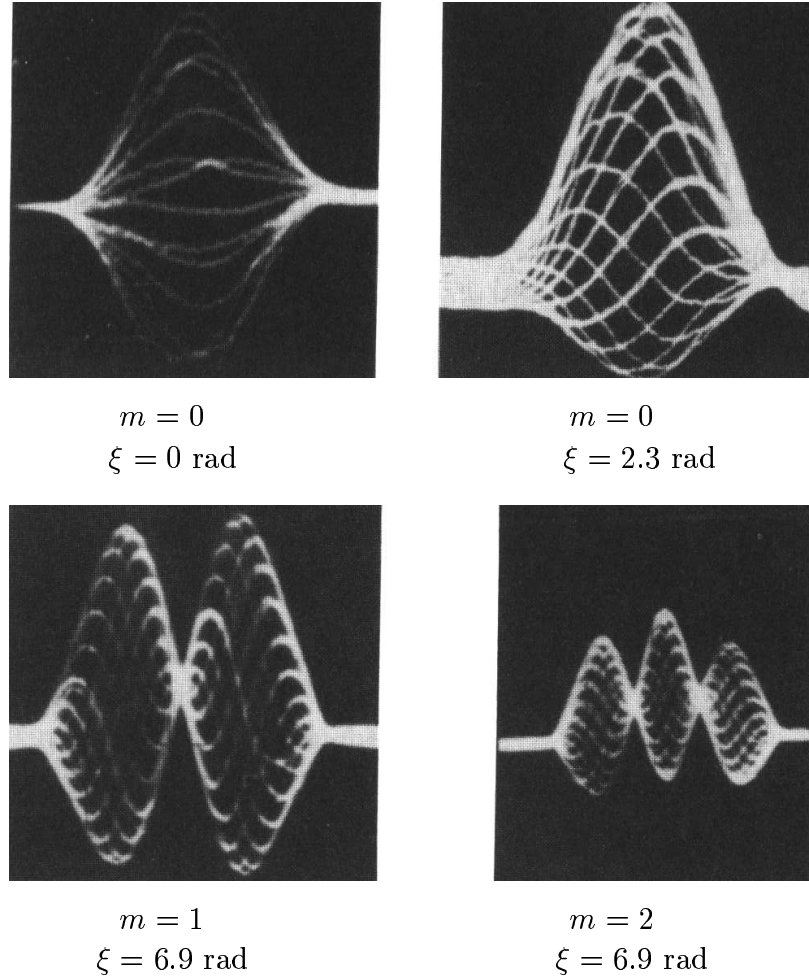


Figure 12.2: A single bunch in the CERN PS Booster monitored in about 20 consecutive revolutions with a wideband pickup (bandwidth  $\sim 150$  MHz). Vertical axis: difference pickup signal. Horizontal axis: time (50 ns per division). The azimuthal mode number and chromaticity in each plot are as labeled.

a nonzero chromaticity breaks the symmetry of the transverse impedance times beam power spectrum between positive and negative frequencies. There is also such an analog in the longitudinal phase space when the synchrotron tune depends on the momentum offset. This comes about because the slip factor  $\eta$  is momentum-offset dependent. In a lattice we can write in general at a certain momentum-offset  $\delta$ ,

$$\eta = \eta_0 + \eta_1\delta + \eta_2\delta^2 + \cdots . \quad (12.9)$$

Usually, because of the small momentum spread  $\delta$ , the contribution of the higher-order terms is small. However, when the operation of the ring is near transition or  $\eta_0 \approx 0$ , most of the contribution of the slippage factor will come from the  $\eta_1$  term. When  $\eta_0$  and  $\eta_1$  are of the same sign, the phase drift of a particle will be larger in one half of the synchrotron oscillation where the momentum spread is positive and smaller in the second half where the momentum spread is negative. The inverse will be true when  $\eta_0$  and  $\eta_1$  have opposite signs. Similar to the transverse situation, this loss of symmetry can excite an instability, which we call longitudinal head-tail instability. In fact, this instability has been observed at the CERN SPS [5] and later at the Fermilab Tevatron. Figure 12.3 shows the output of the rf-bunch phase detector at the CERN SPS, where the bunch length, which was 7 ns at the beginning, is seen increasing for every synchrotron oscillation. This is an instability in the dipole mode with  $\sim 10^{11}$  protons in the bunch. The horizontal scale is 2 s per division or 20 s in total. Thus the growth rate is very slow. To higher order in momentum spread, the off-momentum orbit length can be written as\*

$$C(\delta) = C_0 [1 + \alpha_0\delta(1 + \alpha_1\delta + \alpha_2\delta^2 + \cdots)] , \quad (12.10)$$

with  $C_0 = C(0)$  being the length of the on-momentum orbit. It will be proved in Sec. 18.1 that with the expansion of  $\eta$  in Eq. (12.9), the expressions for the higher-order components of the slip factor are

$$\eta_0 = \alpha_0 - \frac{1}{\gamma^2} , \quad (12.11)$$

$$\eta_1 = \alpha_0\alpha_1 + \frac{3\beta^2}{2\gamma^2} - \frac{\eta_0}{\gamma^2} , \quad (12.12)$$

$$\eta_2 = \alpha_0\alpha_2 + \frac{\alpha_0\alpha_1}{\gamma^2} - \frac{2\beta^4}{\gamma^2} + \frac{3\alpha_0\beta^2}{2\gamma^2} + \frac{\eta_0}{\gamma^4} , \quad (12.13)$$

---

\*In Europe,  $\alpha_0$ ,  $\alpha_1$ ,  $\alpha_2$ , etc. are usually referred to as  $\alpha_1$ ,  $\alpha_2$ ,  $\alpha_3$ , etc. There is also another common definition, where  $C(\delta) = C_0 [1 + \alpha_0\delta + \alpha_1\delta^2 + \alpha_2\delta^3 + \cdots]$ .

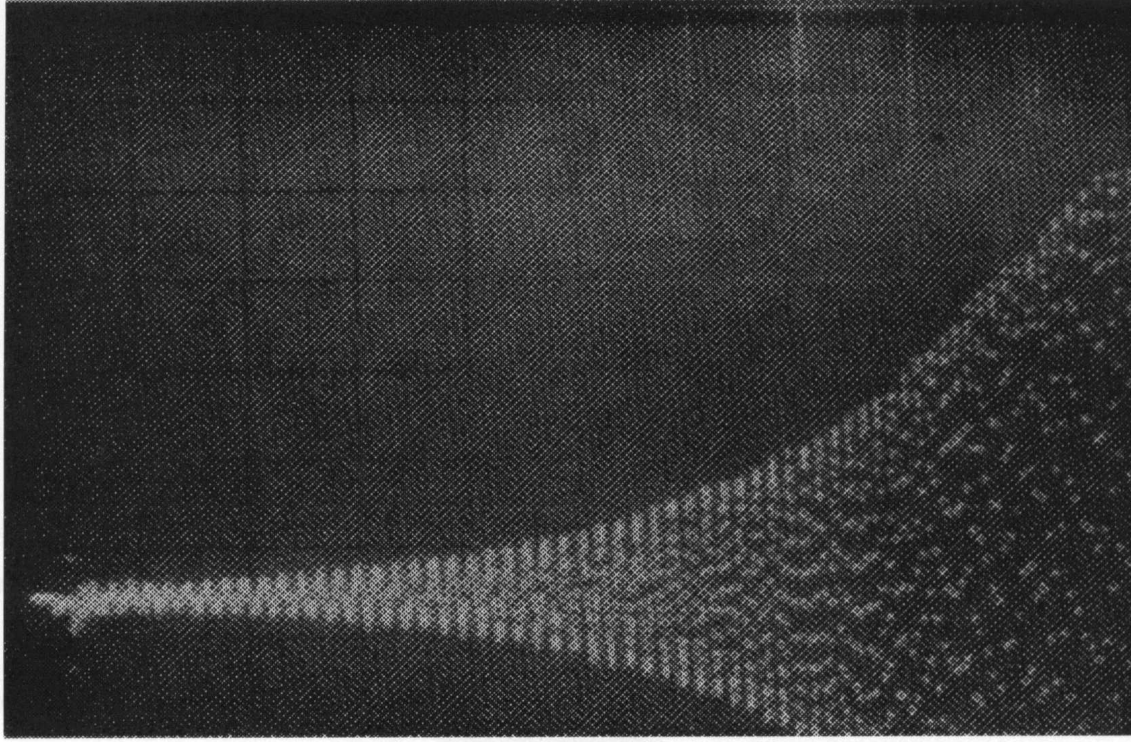


Figure 12.3: Longitudinal head-tail growth of the dipole synchrotron oscillation amplitude recorded from the output of the rf phase detector at the CERN SPS for a bunch with  $\sim 10^{11}$  protons. Horizontal scale is 2 s/div or 20 s total.

where  $\beta$  and  $\alpha$  are the relativistic factors of the synchronous particle. For a high-energy ring like the Fermilab Tevatron, we have almost  $\eta_1 = \alpha_0 \alpha_1$ . For a FODO lattice without special correction,  $\alpha_1$  is positive. Thus, the particle spends more time at positive momentum offset than at negative momentum offset. Then, the bunch becomes relatively longer at positive momentum offset than at negative momentum offset, as is illustrated in Fig. 12.4. The bunch will therefore lose more energy in the lower trajectory than in the upper trajectory. The amplitude of synchrotron oscillation will therefore grow. The energy loss by a beam particle per turn is

$$U(\sigma_\tau) = 2\pi e^2 N_b \int d\omega |\tilde{\rho}(\omega, \sigma_\tau)|^2 \operatorname{Re} Z_0^\parallel(\omega) , \quad (12.14)$$

where  $N_b$  is the number of particles in the bunch, and

$$\tilde{\rho}(\omega, \sigma_\tau) = \frac{1}{2\pi} \int d\tau \rho(\tau, \sigma_\tau) e^{i\omega\tau} \quad (12.15)$$

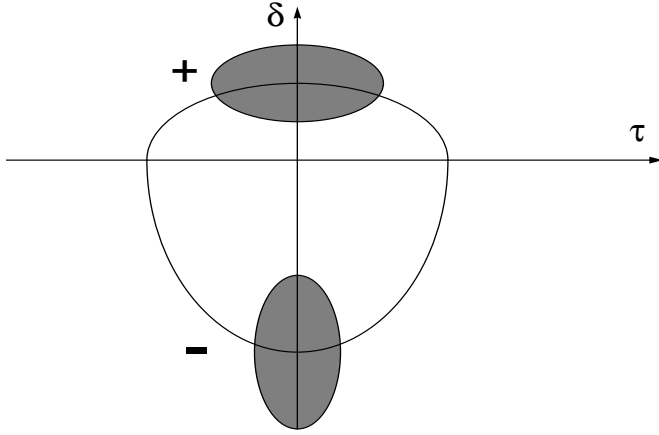


Figure 12.4: A particle trajectory is asymmetric about the on-momentum axis when the slippage factor is not an even function of momentum offset. The bunch will be longer at positive than negative momentum offset when the first-order momentum compaction  $\alpha_0\alpha_1 > 0$  and above transition.

is the spectrum of the bunch of rms length  $\sigma_\tau$  with a distribution  $\rho(\tau, \sigma_\tau)$  normalized to unity. The rms bunch length  $\sigma_\tau$  and the rms energy spread  $\sigma_E$  are related by

$$\omega_s \sigma_\tau = \frac{|\eta| \sigma_E}{\beta^2 E_0}, \quad (12.16)$$

where  $E_0$  is the synchronous energy of the beam and  $\omega_s$  is the small-amplitude synchrotron angular frequency. At the onset of the growth, bunch area is still approximately constant for a proton bunch. Thus, we have

$$\sigma_\tau \propto \sqrt{\frac{|\eta|}{\omega_s}} \propto |\eta|^{1/4} \approx |\eta_0|^{1/4} \left(1 + \frac{\eta_1 \delta}{4\eta_0}\right), \quad (12.17)$$

and

$$\sigma_\tau = \sigma_{\tau 0} \left(1 + \frac{\eta_1 \delta}{4\eta_0}\right), \quad (12.18)$$

where  $\sigma_{\tau 0}$  is the rms bunch length in the absence of the  $\eta_1$  term. The bunch particle gains energy for half a synchrotron period when  $\delta > 0$  and loses energy for the other half synchrotron period when  $\delta < 0$ . Averaging over a synchrotron period, the increase in energy spread per turn is

$$\Delta E = \frac{dU}{d\sigma_\tau} \sigma_\tau \Big|_{\delta>0} - \frac{dU}{d\sigma_\tau} \sigma_\tau \Big|_{\delta<0} = \frac{dU}{d\sigma_\tau} \sigma_{\tau 0} \frac{\delta}{2} \chi, \quad (12.19)$$

where the asymmetry factor  $\chi$  is just the fractional difference in bunch length for  $\delta \gtrless 0$ , and is given, from Eq. (12.18), by

$$\chi = \frac{\eta_1}{\eta_0} = \frac{\alpha_0 \alpha_1 + (\frac{3}{2}\beta^2 - \eta_0)\gamma^{-2}}{\eta_0} \approx \alpha_1 + \frac{3}{2\alpha_0 \gamma^2} \approx \alpha_1 , \quad (12.20)$$

for a proton beam at high energies so that  $\eta_0 \approx \alpha_0$ . In above, Eq. (12.12) has been used and  $\gamma$  and  $\beta$  are the relativistic factors of the synchronous particle. Near transition when  $\alpha_0 \approx \gamma^{-2}$ , however, the asymmetry factor becomes

$$\chi \approx \frac{\alpha_0 \left( \alpha_1 + \frac{3}{2} \right)}{\eta_0} . \quad (12.21)$$

Therefore, this phenomenon is best observed near transition when  $\eta_0$  is small. The time development of the energy spread is given by  $\Delta E \propto e^{t/\tau}$ . The growth rate of the fractional energy spread is therefore [6]

$$\frac{1}{\tau} = -\frac{f_0}{2} \frac{dU}{d\sigma_\tau} \frac{\sigma_{\tau 0}}{\beta^2 E_0} \chi , \quad (12.22)$$

where  $f_0$  is the revolution frequency and  $dU/d\sigma_\tau$  is usually negative. In parallel to the transverse head-tail instability, this instability does not have a threshold although the growth rate is intensity dependent. This instability is essentially a growth of the amplitude of the synchrotron oscillation in the dipole mode. The frequency involved will be the synchrotron frequency. The growth rate is usually very slow. For example, the photo recorded at the CERN SPS, Fig. 12.3 has a horizontal time span of 20 s.

If the driving impedance  $\Re Z_0^\parallel$  comes from a narrow resonance with shunt impedance  $R_s$  at resonant frequency  $\omega_r/(2\pi)$  and quality factor  $Q$ , we have for the energy loss per turn

$$U(\sigma_\tau) = \frac{\pi R_s \omega_r e^2 N_b}{Q} |\tilde{\rho}(\omega_r)|^2 , \quad (12.23)$$

for a bunch containing  $N_b$  particles. For a broadband impedance,  $U(\sigma_\tau)$  drops much faster with bunch length. For a general resonance, we have computed the asymmetric energy loss for a parabolic bunch distribution [7],

$$\begin{aligned} \frac{dU(\sigma_\tau)}{d\sigma_\tau} \sigma_\tau &= \frac{9e^2 N_b \omega_r R_s}{4sQ} \left\{ \frac{2}{z^3} [e^{-2cz} \sin(2sz+2\theta) - \sin 2\theta] \right. \\ &\quad \left. + \frac{4}{z^4} [2e^{-2cz} \sin(2sz+3\theta) + \sin 3\theta] + \frac{12}{z^5} e^{-2cz} \sin(2sz+4\theta) \right\} \end{aligned}$$

$$+ \frac{6}{z^6} [e^{-2cz} \sin(2sz + 5\theta) - \sin 5\theta] \Big\} , \quad (12.24)$$

where  $z = \sqrt{5}\omega_r\sigma_\tau$ ,  $c = \cos\theta = 1/(2Q)$ , and  $s = \sin\theta$ . This is plotted in Fig. 12.5 for the case of a sharp resonance and in Fig. 12.6 for the case of a broadband with  $Q = 1$ .

As is shown in Fig. 12.5, the asymmetric energy loss vanishes when the bunch length goes to zero, because the change in bunch length from positive momentum offset to negative momentum offset also goes to zero. On the other hand, when the bunch length is very long, the asymmetric energy loss will also be small, because the energy loss for a long bunch is small.

Let us apply the theory to the Fermilab Tevatron in the collider mode [7]. The asymmetric factor in Eq. (12.20) has been measured to be  $\chi \sim +1.17$ . The fundamental resonance of the 8 rf cavities serves as a good driving force for this instability. Each cavity has resonant frequency  $f_r = 53.1$  MHz,  $R_s = 1.2$  MΩ, and  $Q = 7000$ . For Run I, where the rms bunch length was  $\sigma_\tau \approx 2.684$  ns or  $f_r\sigma_\tau \approx 0.1425$ ,  $(dU/d\sigma_\tau)\sigma_\tau \sim -0.3890 e^2 N_b \omega_r R_s / Q$  is large and leads to a growth rate of  $\tau^{-1} = 1.433 \times 10^{-3}$  s<sup>-1</sup> at the injection energy of  $E_0 = 150$  GeV for a bunch containing  $N_b = 2.70 \times 10^{11}$  particles. However, for Run II, the bunch will be much shorter. With  $\sigma_\tau = 1.234$  ns or  $f_r\sigma_\tau \approx 0.0655$ , the asymmetric energy loss  $(dU/d\sigma_\tau)\sigma_\tau \sim -0.1464 e^2 N_b \omega_r R_s / Q$  is much smaller and the head-tail growth rate becomes  $\tau^{-1} = 0.539 \times 10^{-3}$  s<sup>-1</sup>. As is shown in Fig. 12.5, we are on the left side of the  $(dU/d\sigma_\tau)\sigma_\tau$  peak; therefore a shorter bunch length leads to slower growth.

The broadband impedance can also have similar contributions since the resonance frequency is usually a few GHz and  $\Re Z_0^\parallel$  is large although  $Z_0^\parallel/n$  is just a couple of ohms. Now  $\omega_r\sigma_\tau$  falls on the right side of the  $(dU/d\sigma_\tau)\sigma_\tau$  peak instead. We expect shorter bunch lengths to have faster growth rates, as is indicated in Fig. 12.6. Table 12.2 shows the longitudinal head-tail growth rates for different resonant frequencies and quality factors;  $Z_0^\parallel/n = 2 \Omega$  has been assumed. The growth rates driven by the fundamental rf resonance are also listed in the last row for comparison. It is obvious that the longitudinal head-tail instability for Run I is dominated by the rf narrow resonance and that for Run II by the broadband impedance instead. We observed a growth time of  $\sim 250$  s in Run I. From Table VI, it is very plausible that the growth of this head-tail instability will be at least as fast as that in Run I.

Let us go back to the observation at the CERN SPS. The bunch has a synchronous momentum of 26 GeV/c. The transition gamma is  $\gamma_t = 23.4$ , giving  $\eta = 5.26 \times 10^{-4}$ . For

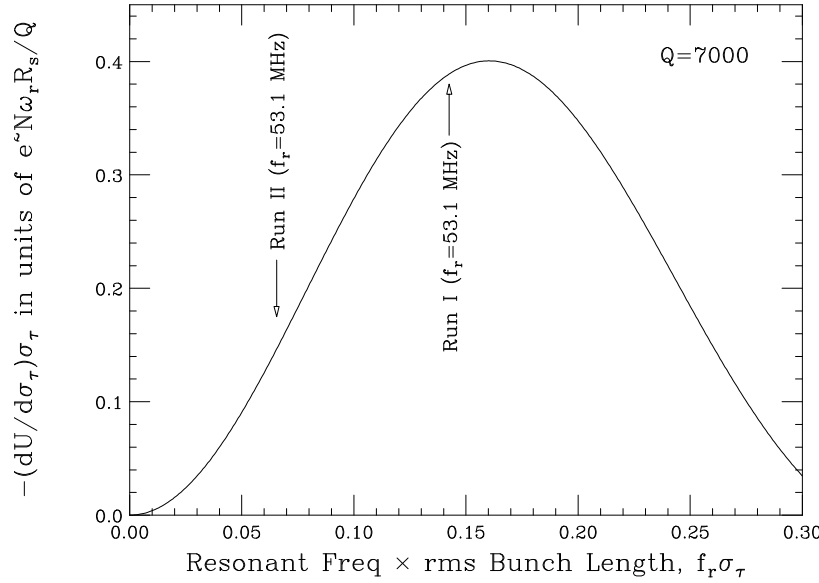


Figure 12.5: Plot of differential bunch energy loss  $(dU/d\sigma_\tau)\sigma_\tau$  versus  $f_r\sigma_\tau$  due to a sharp resonance. Note that the effect on the Run II bunch is much less than that on the Run I bunch because of the shorter Run II bunch length.

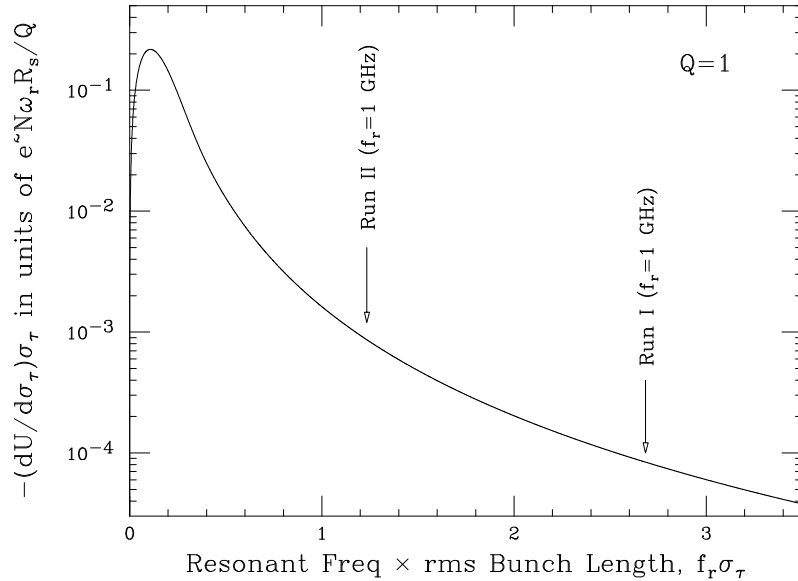


Figure 12.6: Plot of differential bunch energy loss  $(dU/d\sigma_\tau)\sigma_\tau$  versus  $f_r\sigma_\tau$  due to a broadband resonance with  $Q = 1$ . Note that the effect on the Run II bunch is much more than that on the Run I bunch because of the shorter Run II bunch length.

Table 12.2: Growth rates for a broadband resonance of  $Z_0^{\parallel}/n = 2 \Omega$  at various frequencies and quality factors.

$f_r$ (GHz)	$Q$	Growth Rate ( $s^{-1}$ )	
		Run I	Run II
1	1	$0.178 \times 10^{-3}$	$1.829 \times 10^{-3}$
1	3	$0.022 \times 10^{-3}$	$0.267 \times 10^{-3}$
2	1	$0.089 \times 10^{-3}$	$0.915 \times 10^{-3}$
2	2	$0.023 \times 10^{-3}$	$0.249 \times 10^{-3}$
1	5	$0.009 \times 10^{-3}$	$0.114 \times 10^{-3}$
2	3	$0.011 \times 10^{-3}$	$0.117 \times 10^{-3}$
2	4	$0.006 \times 10^{-3}$	$0.070 \times 10^{-3}$
Fundamental Rf Resonance		$1.433 \times 10^{-3}$	$0.539 \times 10^{-3}$

the horizontal chromaticity setting used during the observation of the longitudinal head-tail growth in Fig. 12.3, a lattice-code simulation program gives the next higher-order component of the momentum compaction to be  $\alpha_1 = -0.7$ . The asymmetry parameter turns out to be  $\chi = 1.28$ . We therefore expect an instability if  $dU/d\sigma_{\tau} < 0$  which is normally the case. In other words, to observe such an instability, one should perform the experiment above transition, but not too much above transition so as to enhance the asymmetry parameter  $\chi$ .

The longitudinal head-tail instability can also be driven by the resistive wall impedance. The differential energy loss in Eq (12.20) integrates to

$$\frac{dU}{d\sigma_{\tau}} \sigma_{\tau} = -\frac{3\Gamma(\frac{3}{4})}{8\pi^2} \frac{e^2 N_b [\Re Z_{\parallel}]_1}{\omega_0^{1/2} \sigma_{\tau}^{3/2}}, \quad (12.25)$$

where

$$[\Re Z_{\parallel}]_1 = \frac{R\rho}{b\delta_1} \quad (12.26)$$

is the resistive part of the wall impedance at revolution frequency. The skin depth at revolution frequency is

$$\delta_1 = \sqrt{\frac{2\rho}{\mu_0 \mu_r \omega_0}}, \quad (12.27)$$

where  $\mu_r$  is the relative magnetic permeability and  $\rho$  is the electric resistivity of the beam pipe.  $\Gamma(\frac{3}{4}) = 1.2254167$  is the Gamma function at  $\frac{3}{4}$ . Because of the  $\sigma_{\tau}^{3/2}$  in the denominator, the contribution can be important for very short bunches.

The longitudinal head-tail instability can be important in quasi-isochronous storage rings, because the the asymmetric factor as defined in Eq. (12.21) can become very large when the ring operation is close to transition. Such rings have been designed for the muon colliders. An isochronous ring is preferred because the muon bunches will be short, roughly 3 mm, which requires an rf voltage in the 50 MV range [8]. Such an rf system will be very expensive. In most of these designs, the muons only have a lifetime of about 1000 turns. If the ring is quasi-isochronous, even without rf, the debunching will be rather insignificant. In order not to degrade the luminosity of the collider, however, one must make sure that the growth time of the longitudinal head-tail instability will be much longer than 1000 turns.

## 12.3 Exercises

- 12.1. The degrees of freedom of a system are coupled internally. Some degrees of freedom continue to gain energy and grow while some lose energy and are damped. When the system is not getting energy from outside, the sum of the damping or antidamping rates of all degrees of freedom must add up to zero. If the head-tail stability or instability for all azimuthal modes do not draw energy from outside, energy must be conserved, or

$$\sum_{m=0}^{\infty} \frac{1}{\tau_m} = 0 , \quad (12.28)$$

where  $\tau_m^{-1}$  is given by Eq. (12.1), independent of chromaticity and the detail of the transverse impedance. Show that Eq. (12.28) is only satisfied if the factor  $(1+m)^{-1}$  in Eq. (12.1) is removed. We may conclude that either the factor  $(1+m)^{-1}$  should not be present in Sacherer's formula or this is not an internal system.

Hint: Show that  $\sum_m |h_m(\omega)|^2$  is a constant independent of  $\omega$  by performing the summation numerically. This follows from the fact that the modes of excitation  $\lambda_m(\tau)$  form a complete set. Then the integration over  $\mathcal{R}e Z_1^\perp(\omega_0)$  gives zero.

- 12.2. In an isochronous ring or an ultra-relativistic linac<sup>†</sup>, the particle at the head of the bunch will not exchange position with the particle at the tail. Thus the particle at the tail suffers from the wake of the head all the time. We can consider a macro-particle model with only two macro-particles, each carrying charge  $eN/2$  and separated by a distance  $\hat{z}$  longitudinally. The head particle executes a free betatron oscillation

$$y_1(s) = \hat{y} \cos k_\beta s , \quad (12.29)$$

while the tail sees a deflecting wake force  $\langle F_1^\perp \rangle = e^2 N W_1(\hat{z}) y_1(s)/(2\ell)$  and its transverse motion is determined by

$$y_2'' + k_\beta^2 y_2 = -\frac{e^2 N W_1(\hat{z})}{2E_0 \ell} , \quad (12.30)$$

where  $k_\beta = \omega_\beta/v$  is the betatron wave number,  $\ell$  is the length of the vacuum chamber that supplies the wake. If one prefers, one can define  $W_1$  as the wake

---

<sup>†</sup>For all the proton linacs in existence, the highest energy is less than 1 GeV, or proton velocity less than 0.875 of the velocity of light. Thus, normal synchrotron motion takes place, implying that head and tail of a bunch do exchange position. Therefore, Exercise 12.2 applies mostly to electron linacs.

force integrated over one rf-cavity period; then  $\ell$  will be the length of the cavity period. Show that the solution of Eq. (12.30) is

$$y_2(s) = \hat{y} \left[ \cos k_\beta s - \frac{e^2 N W_1(\hat{z})}{4k_\beta E_0 \ell} s \sin k_\beta s \right]. \quad (12.31)$$

The second term is the resonant response to the wake force and grows linearly. Show that the total growth in transverse amplitude along a length  $\ell_0$  of the linac relative to the head particle is

$$\Upsilon = -\frac{e^2 N W_1(\hat{z}) \ell_0}{4k_\beta E_0 \ell}. \quad (12.32)$$

The above mechanism is called beam breakup.

- 12.3. Derive the asymmetric energy loss,  $[dU(\sigma_\tau)/d\sigma_\tau]\sigma_\tau$  as given by Eq. (12.24) of a particle in a bunch with linear parabolic distribution driven by a resonance.



# Bibliography

- [1] F.J. Sacherer, *Theoretical Aspects of the Behaviour of Beams in Accelerators and Storage Rings*, Proc. First Course of Int. School of Part. Accel., Erice, Nov. 10-22, 1976, p.198.
- [2] C. Pellegrini, Nuovo Cimento **64**, 447 (1969).
- [3] M. Sands, SLAC-TM-69-8 (1969).
- [4] K. Hübner, P. Strolin, V. Vaccaro, and B. Zotter, *Concerning the Stability of the ISR Beam Against Coherent Dipole Oscillations*, CERN/ISR-RF-TH/70-2 (1970).
- [5] D. Boussard and T. Linnecar, Proc. 2nd EPAC, Nice, 1990, ed. Marin and Mandrillon, p.1560.
- [6] B. Chen, *The Longitudinal Collective Instabilities of Nonlinear Hamiltonian Systems in a Circular Accelerator*, Thesis, U. of Texas at Austin, May, 1995.
- [7] K.Y. Ng, *Impedances and Collective Instabilities of the Tevatron at Run II*, Fermilab report TM-2055, 1998.
- [8] King-Yuen Ng *Quasi-Isochronous Buckets in Storage Rings*, Nucl. Inst. Meth. **A404**, 199 (1988).

